International Journal of Heat and Mass Transfer 122 (2018) 222–228

Contents lists available at ScienceDirect

International Journal of Heat and Mass Transfer

journal homepage: www.elsevier.com/locate/ijhmt

Computational analysis of three layer fluid model including a nanomaterial layer

D.C. Lu [a], U. Farooq [a,b,*], T. Hayat [c,d], M.M. Rashidi [e], M. Ramzan [f,g]

[a] School of Sciences, Jiangsu University, Zhenjiang, China
[b] Department of Mathematics, COMSATS Institute of Information Technology, Park Road, Tarlai Kalan, Islamabad 44000, Pakistan
[c] Department of Mathematics, Quaid.i.Azam University, Islamabad 44000, Pakistan
[d] Nonlinear Analysis and Applied Mathematics (NAAM) Research Group, Department of Mathematics, Faculty of Science, King Abdulaziz University, P.O. Box 80203, Jeddah 21589, Saudi Arabia
[e] Department of Civil Engineering, University of Birmingham, Edgbaston, B15 2TT Birmingham, United Kingdom
[f] Department of Computer Science, Bahria University, Islamabad Campus, Islamabad 44000, Pakistan
[g] Department of Mechanical Engineering, Sejong University, Seoul 143-747, Republic of Korea

ARTICLE INFO

Article history:
Received 16 August 2017
Received in revised form 17 November 2017
Accepted 18 January 2018

Keywords:
BVPh2.0
Multi-layer flow
Optimal homotopy analysis method
Nanofluids
Nonlinear heat transfer
Reversed flow

ABSTRACT

Multi-layer flows regime occurs in many industrial processes such as petroleum and chemical industry, therefore the study of multi-layer flow in the presence of nanoparticles can be used to obtain desired qualities. This article investigates a vertical three-layer fluid model which incorporates two clear fluid layers and a nanofluid layer which is squeezed between them. A fully developed laminar, incompressible flow field is considered including viscous dissipation effects. The present framework is formulated by capitalizing Buongiorno model which integrate the combined effects of thermophoresis and Brownian motion. The set of ordinary differential equations (ODEs) are non-dimensionalized under appropriate transformations and a nonlinear differential system is than solved by BVPh2.0 solver which is based on an analytical technique named as homotopy analysis method (HAM). Based on the average squared residual error, a procedure for the highly accurate approximation is developed in BVPh2.0. For generalized set of physical parameters it is demonstrated that our obtained solutions are convergent. The influences of governing parameters on the temperature, flow and concentration are analyzed. The result shows a reversed flow for higher values of mixed convection parameter. Furthermore the flow and temperature characteristics at the interface for thermophoresis and Brownian motion parameters are examined numerically.

1. Introduction

Heat and mass transfer is an important process in many industrial applications. The conventional fluids for example ethylene glycol mixtures, water and oil have naturally poor thermal conductivity. This imposes a key restriction on the efficient heat transfer. In recent years significant research activity has been made for the optimization of the performance of heat transfer fluids. In order to increase the thermal conductivity Maxwell [1] used mettalic particles, many other scientists experimented by inserting particles of micrometer- or milimeter-size respectively in the base fluid but due to the particle size major problem arouse in their settlement. The term nanofluid is first used by Choi [2]. These fluids are synthesized by the suspension of nanometer sized solid particles and fibers. Nanometer sized particles can be mettalic, polymeric or non-mettalic etc. Thus the characteristics associated with heat transfer can be greatly improved by the suspension of these particles in the original fluid. These particles are thus suspended in the base fluid to improve heat transfer characteristics of the original fluid. Therefore these particles are quite useful in improving the performance of the ordinary liquids. Nanofluids are significant in many industrial processes such as microelectronics, hybrid powered engines, pharmaceutical processes, air conditioning industry, improved oils, coolants and so on. The comprehensive review of convective transport in nanofluids comprise the attempts of Buongiorno [3], Kuzentsov and Nield [4], Wang and Mujamdar [5] and Das et al. [6]. Few other studies on nanofluids can be referred in the following Refs. [7–18].

* Corresponding author at: School of Sciences, Jiangsu University, Zhenjiang, China.
E-mail addresses: umer_farooq@comsats.edu.pk (U. Farooq), tahaksag@yahoo.com (T. Hayat).

https://doi.org/10.1016/j.ijheatmasstransfer.2018.01.080
0017-9310/

Heat transfer and mixed convection associated with fluid flow in channels has been the subject of many studies because of its immense utilization in the projects of cooling system for electronic machines, nuclear reactors, solar energy collection and so on. Numerous research works have been focused on mixed convective flows of one-layer fluid model in vertical channels under different physical conditions. Tao [19], Aung and Worku [20] and Kimura et al. [21] did pioneering work in the mixed convection flows under different conditions. Afterwards extensive research work is presented on mixed convection flows. Some recent research articles on mixed convection flows of nanofluids can be stated through Refs. [22–34]. Realistically the fluid models of multi-layers are important in the understanding of fluid unifications and their influence on momentum and heat transfer properties. In reality a number of times transport phenomena occur at the interface in non-isothermal systems of fluids with different layers. The study of two layer model is important because of its application in the fluid experiments which are conducted in such an environment where gravitational force is low. Umavathi et al. [35] considered a porous-clear fluid flow model in a horizontal channel. Robert et al. [36] investigated a two layer model in the vertical channel. One layer contains clear fluid and the other layer contains nanofluid. Umer and Lin [37] proposed physically more appropriate non-dimensional definitions for the governing parameters. The results showed that the flow is reversed when the value of the buoyancy parameter is sufficiently high. Umer et al. [38] extended the two layer model for the non-Newtonian third grade fluid. Vajravelu et al. [39] extended the two layer moder of Robert et al. [36] to the three layer fluid. Three layer model is investigated by Umavathi et al. [40]. Here middle layer contains the porous media and the other two layers are filled with clear fluid. Since multi-layer fluid models have wide range of applications in the industry and natural environment therefore the aim of this article is to analyze three layer fluid model.

There is a large number of research papers related to HAM [41]. It is because of its efficiency in solving differential equations. More importantly unlike other analytical methods it provides us an easy way to determine the convergence of our results for the solution of non-linear differential equations by introducing parameters which are known as convergence enhancing parameters. The HAM has been already employed successfully to numerous problems from engineering, science, and finance (see for instance [42–44]). Liao [45] further improved the HAM by introducing optimal convergence control parameters. In order to make it convenient for the users Liao developed HAM-based solvers in Mathematica and Maple. The most recent and powerful of them is BVPh2.0 which is online available at (http://numericaltank.sjtu.edu.cn/BVPh.htm). BVPh2.0 has been successfully used by different researchers [46–50] in the solutions of highly non-linear set of ordinary differential sytems.

Here we intend to carry out analysis for the heat transfer and flow properties of a three layer fluid model using BVPh2.0 solver. A vertical channel is divided into three layers. The middle layer is filled with nanofluid and the other two layers contain clear fluids. The system of seven coupled non-linear ODEs is solved by BVPh2.0. The interface boundary conditions (BCs) are easy to handle in the frame work of OHAM because of its utilization of functions instead of numbers. BVPh2.0 ensures the convergence of the solutions by the average squared residual error for individual equation and hence for the whole system. Furthermore the heat and mass transfer properties for different values of the physical parameters have been analyzed. The results indicate that the nanoparticle concentration in the original fluid can remarkably improve heat and mass transfer characteristics.

2. Problem formulation

Fig. 1 consists of flow configuration of the problem under consideration. The infinite plates in the $x-$ and $z-$directions, respectively are parallel to each other. The middle layer contains nanofluid and the other two layers contain clear fluid. The clear fluid regions $-h \leqslant y \leqslant 0$ and $h \leqslant y \leqslant 2h$ have density ρ_1, viscosity μ_1 and thermal diffusivity α_1. The nanofluid region $0 \leqslant y \leqslant h$ has density ρ_2, viscosity μ_2 and thermal diffusivity α_2. It is assumed that the temperature at both walls is different. Right/Left walls have temperatures T_{w1}/T_{w2} with the assumption $(T_{w2} < T_{w1})$. The fluid flow is taken as laminar, steady and the fluid characteristics are supposed to be constant. The governing equations are given by

Region-I

$$\nu_1 \frac{d^2u_1}{dy^2} - \frac{1}{\rho_1}\frac{dp}{dx} + g\beta_1(T_1 - T_{w2}) = 0, \tag{1}$$

$$\alpha_1 \frac{d^2T_1}{dy^2} + \frac{Q_1}{\rho_1 C_p}(T_1 - T_{w2}) + \frac{\mu_1}{\rho_1 C_p}\left(\frac{du_1}{dy}\right)^2 = 0. \tag{2}$$

Region-II

$$\nu_2 \frac{d^2u_2}{dy^2} - \frac{1}{\rho_2}\frac{dp}{dx} + g\beta_2(T_2 - T_{w2}) = 0, \tag{3}$$

$$\alpha_2 \frac{d^2T_2}{dy^2} + \tau\left[D_B\frac{dC}{dy}\frac{dT_2}{dy} + \frac{D_T}{T_{w2}}\left(\frac{dT_2}{dy}\right)^2\right] + \frac{Q_2}{\rho_2 C_p}(T_2 - T_{w2}) + \frac{\mu_2}{\rho_2 C_p}\left(\frac{du_2}{dy}\right)^2 = 0, \tag{4}$$

$$D_B\frac{d^2C}{dy^2} + \frac{D_T}{T_{w2}}\frac{d^2T_2}{dy^2} = 0. \tag{5}$$

Region-III

$$\nu_1 \frac{d^2u_3}{dy^2} - \frac{1}{\rho_1}\frac{dp}{dx} + g\beta_1(T_3 - T_{w2}) = 0, \tag{6}$$

$$\alpha_1 \frac{d^2T_3}{dy^2} + \frac{Q_3}{\rho_1 C_p}(T_3 - T_{w2}) + \frac{\mu_1}{\rho_1 C_p}\left(\frac{du_3}{dy}\right)^2 = 0. \tag{7}$$

Here, u_i and v_i are $x-$ and $y-$components of the fluid respectively, where $i = 1, 2, 3$. $C, T_i, Q_i, \nu_i, \beta_i, D_T, g, C_p, D_B$ and $\tau = (\rho C_p)_p/(\rho C_p)_f$ denote nanoparticle volume fraction, temperature, internal heat generation or absorption, kinematic viscosity,

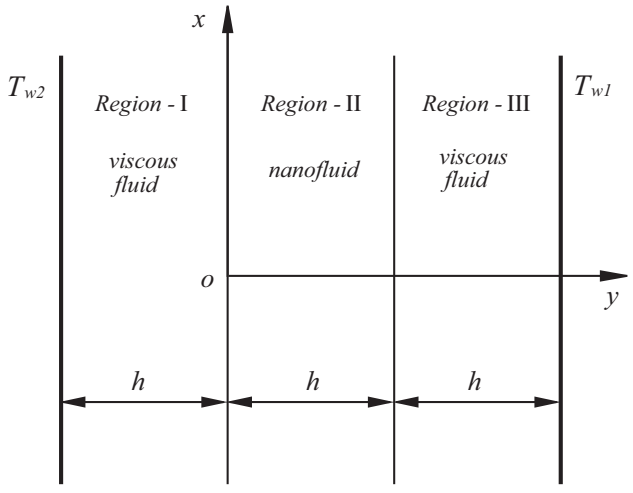

Fig. 1. Physical configuration.

coefficient of thermal expansion, thermophoretic diffusion coefficient, gravity acceleration, specific heat at constant pressure, Brownian diffusion coefficient and heat capacity ratio, respectively. The subscripts p represents nanoparticles and f represents base fluid.

The temperatures, velocities, shear stresses and the heat fluxes are assumed to be continuous at the interfaces. The no-slip and isothermal BCs are used for the velocity and temperature, respectively. Thus the BCs are:

$$\begin{aligned}
&u_1(y)=0, \quad T_1(y)=T_{w2}, \quad \text{at } y=-h,\\
&\left.\begin{aligned}&u_1(y)=u_2(y), \quad T_1(y)=T_2(y), \quad C(y)=C_w,\\ &\mu_1\tfrac{du_1}{dy}=\mu_2\tfrac{du_2}{dy}, \quad \alpha_1\tfrac{dT_1}{dy}=\alpha_2\tfrac{dT_2}{dy},\end{aligned}\right\} \quad \text{at } y=0,\\
&\left.\begin{aligned}&u_2(y)=u_3(y), \quad T_2(y)=T_3(y), \quad C(y)=0,\\ &\mu_2\tfrac{du_2}{dy}=\mu_1\tfrac{du_3}{dy}, \quad \alpha_2\tfrac{dT_2}{dy}=\alpha_1\tfrac{dT_3}{dy},\end{aligned}\right\} \quad \text{at } y=h,\\
&u_3(y)=0, \quad T_3(y)=T_{w1}, \quad \text{at } y=2h.
\end{aligned} \tag{8}$$

Choosing

$$\begin{aligned}
&y^*=\frac{y}{h}, \quad u_1^*=\frac{u_1}{\tilde{u}}, \quad u_3^*=\frac{u_3}{\tilde{u}}, \quad u_2^*=\frac{u_2}{\tilde{u}}, \quad \theta_1=\frac{T_1-T_{w2}}{T_{w1}-T_{w2}},\\
&\theta_2=\frac{T_2-T_{w2}}{T_{w1}-T_{w2}},\\
&\theta_3=\frac{T_3-T_{w2}}{T_{w1}-T_{w2}}, \quad \phi=\frac{C}{C_w}, \quad P_1=-\frac{h^2}{\mu_1\tilde{u}}\frac{\partial p}{\partial x}, \quad P_2=-\frac{h^2}{\mu_2\tilde{u}}\frac{\partial p}{\partial x},\\
&Gr_1=\frac{g\beta_1(T_{w1}-T_{w2})h^3}{\nu_1^2},
\end{aligned} \tag{9}$$

$$Gr_2=\frac{g\beta_2(T_{w1}-T_{w2})h^3}{\nu_2^2}, \quad Re_1=\frac{\tilde{u}h}{\nu_1}, \quad Re_2=\frac{\tilde{u}h}{\nu_2},$$

the dimensionless equations after suppressing the asterisks for brevity are reduced as follows:

Region-I

$$\frac{d^2u_1}{dy^2}+P_1+\lambda_1\theta_1=0, \tag{10}$$

$$\frac{d^2\theta_1}{dy^2}+Pr_1\left[\delta_1\theta_1+Ec\left(\frac{du_1}{dy}\right)^2\right]=0, \tag{11}$$

Region-II

$$\frac{d^2u_2}{dy^2}+P_2+\lambda_2\theta_2=0, \tag{12}$$

$$\frac{d^2\theta_2}{dy^2}+Pr_2\left[N_b\frac{d\theta_2}{dy}\frac{d\phi}{dy}+N_t\left(\frac{d\theta_2}{dy}\right)^2+\delta_2\theta_2+Ec\left(\frac{du_2}{dy}\right)^2\right]=0, \tag{13}$$

$$\frac{d^2\phi}{dy^2}+\frac{N_t}{N_b}\frac{d^2\theta_2}{dy^2}=0, \tag{14}$$

Region-III

$$\frac{d^2u_3}{dy^2}+P_1+\lambda_1\theta_3=0, \tag{15}$$

$$\frac{d^2\theta_3}{dy^2}+Pr_1\left[\delta_3\theta_3+Ec\left(\frac{du_3}{dy}\right)^2\right]=0, \tag{16}$$

where the parameters N_b, λ, Pr, N_t and Ec are Brownian motion parameter, mixed convection parameter, the Prandtl number, the thermophoresis parameter and the Eckert number, respectively. These are defined by

$$\lambda_1=\frac{Gr_1}{Re_1^2}, \quad \lambda_2=\frac{Gr_2}{Re_2^2}, \quad Pr_1=\frac{\nu_1}{\alpha_1}, \quad Pr_2=\frac{\nu_2}{\alpha_2}, \quad Ec=\frac{\tilde{u}^2}{C_p(T_{w1}-T_{w2})}, \tag{17}$$

$$N_b=\frac{\tau D_B C_w}{\nu_2}, \quad N_t=\frac{\tau D_T(T_{w1}-T_{w2})}{\nu_2 T_{w2}},$$

and the $\delta_i (i=1-3)$ represent heat sink or source in the regions-I, -II and -III, respectively. We have

$$\delta_1=\frac{Q_1h^2}{\rho_1C_p\nu_1}, \quad \delta_2=\frac{Q_2h^2}{\rho_2C_p\nu_2}, \quad \delta_3=\frac{Q_3h^2}{\rho_1C_p\nu_1},$$

with

$$d_1=\frac{\alpha_2}{\alpha_1}, \quad m_1=\frac{\mu_1}{\mu_2}.$$

Dimensionless BCs become

$$\begin{aligned}
&u_1(y)=0, \quad \theta_1(y)=0, \quad \text{at } y=-1,\\
&\left.\begin{aligned}&u_1(y)=u_2(y), \quad \theta_1(y)=\theta_2(y), \quad \phi(y)=1,\\ &\tfrac{du_1}{dy}=\tfrac{1}{m_1}\tfrac{du_2}{dy}, \quad \tfrac{d\theta_1}{dy}=\tfrac{1}{d_1}\tfrac{d\theta_2}{dy},\end{aligned}\right\} \quad \text{at } y=0,\\
&\left.\begin{aligned}&u_2(y)=u_3(y), \quad \theta_2(y)=\theta_3(y), \quad \phi(y)=0,\\ &\tfrac{du_2}{dy}=m_1\tfrac{du_3}{dy}, \quad \tfrac{d\theta_2}{dy}=d_1\tfrac{d\theta_3}{dy},\end{aligned}\right\} \quad \text{at } y=1,\\
&u_3(y)=0, \quad \theta_3(y)=1, \quad \text{at } y=2.
\end{aligned} \tag{18}$$

The relation defining mass flux conservation in the channel are as follows:

$$\int_{-1}^{0}u_1(y)\,dy=1. \tag{19}$$

$$\int_{0}^{1}u_2(y)\,dy=1. \tag{20}$$

$$\int_{1}^{2}u_3(y)\,dy=1. \tag{21}$$

3. Results and discussion

It should be pointed out that the HAM based solutions contain convergence enhancing parameters. These parameters play vital role in getting convergent solutions.

BVPh2.0 solver is used to analyze a three layer fluid model. The Prandtl numbers (Pr_1), (Pr_2), ratio of viscosities (m_1), ratio of thermal diffusivities (d_1) and non-dimensional heat generation/absorption (δ_i) in all the regions are chosen to be $7.0, 1.0, 0.5$, 0.5 and -0.1 respectively, throughout the computations. We choose $Pr_1=7.0, Pr_2=1.0, Ec=0.1, \lambda=0.5$, $\delta_1=\delta_2=\delta_3=-0.1$, $m_1=d_1=0.5, N_b=0.5, N_t=0.1$. To save computation time we set $c_0^{u_1}=c_0^{u_2}=c_0^{u_3}=h_1$, $c_0^{\theta_1}=c_0^{\theta_2}=c_0^{\theta_3}=h_2$. The optimized values for the convergence enhancing parameters at various orders of iterations are obtained by employing the command "**GetOptiVar**. The objective here is to get the optimal values of the convergence enhancing parameters by reducing the total error. The average residual errors for each equation and total residual error for whole system is shown in Table 1. The values for average residual errors and the value of the total squared residual errors are reducing as the order of iteration is increasing.

The effects of thermophoresis (N_t) and Brownian motion (N_b) parameters on the velocity and temperature profiles at the interface are shown in the Tables 2 and 3. The mixed convection parameters $\lambda>0$, $\lambda<0$ and $\lambda=0$ correspond to the fluid heating, fluid cooling and absence of mixed convection effects, respectively. For $\lambda=0$ the increase in the values of N_b and N_t doesnot change the velocity profiles. However for the fluid heating case that is $\lambda=0.5$, an increase in N_t keeping N_b fixed decelerate the flow rate at the interface. An increase in N_b keeping N_t fixed decreases the

Table 1
Individual and total residual errors when $h_1 = -0.98, h_2 = -0.84, c_0^{\phi} = -1.02$.

m	10	20	30
$\mathscr{E}_m^{u_1}$	4.29×10^{-15}	1.71×10^{-27}	3.26×10^{-32}
$\mathscr{E}_m^{\theta_1}$	4.29×10^{-15}	4.15×10^{-27}	1.61×10^{-30}
$\mathscr{E}_m^{u_2}$	6.23×10^{-15}	1.73×10^{-27}	2.00×10^{-33}
$\mathscr{E}_m^{\theta_2}$	1.84×10^{-13}	8.56×10^{-26}	9.62×10^{-34}
$\mathscr{E}_m^{\phi}$	6.02×10^{-14}	2.63×10^{-26}	8.67×10^{-34}
$\mathscr{E}_m^{u_3}$	7.25×10^{-15}	4.24×10^{-27}	3.43×10^{-28}
$\mathscr{E}_m^{\theta_3}$	5.50×10^{-15}	3.71×10^{-27}	1.2×10^{-27}
$\mathscr{E}_m^{t}$	2.72×10^{-13}	1.27×10^{-25}	1.55×10^{-27}

velocity profiles. Therefore we may conclude that the velocity profiles can be controlled by adding nanoparticles in basefluid.

From Table 3 it is shown for $\lambda = 0$ that the increase in N_t keeping N_b fixed enhances the temperature. Large temperature show an increase in the temperature difference between the adjacent fluid and the wall. Temperature profile is reduced considerably for higher N_b. It is indeed interesting to point out that in nanofluids the existence of Brownian motion is because of particle size. When the size of the particle approaches the nanometer scale, the Brownian motion is an important factor in the heat transfer. For assisting case the increase in the values of either N_t or N_b decreases the temperature at the interface.

Figs. 2–7 depict the graphs of concentration, velocity and temperature profiles. The analysis of the graphs for various values of Eckert number, mixed convection and thermophoresis parameters are presented.

Variations of velocity profile as a function of y for a wide of λ are plotted in Fig. 2. The flow is reversed through out the channel. It is noted that the increased buoyancy increases flow near right wall

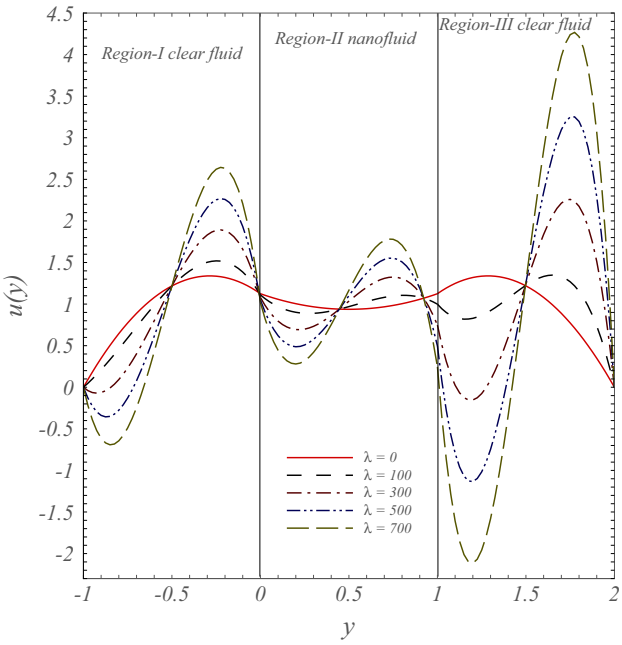

Fig. 2. Velocity profiles for various values of λ.

and it decreases adjacent to interface in the clear fluid region. It can be seen from the nanofluid region that the effects of nanoparticle is to decelerate the flow therefore for flow assisting case N_b and N_t opposes the transport phenomena in the nanofluids region. Here the BVPh2.0 results validate the results of Aung and Worku [20]. From mathematical point of view Fig. 3 depicts initially

Table 2
Velocity characteristics at the interface when iteration order is 50.

λ			$\frac{du_1}{dy}(-1)$	$u_1(0)$	$\frac{du_1}{dy}(0)$	$u_2(1)$	$\frac{du_2}{dy}(1)$
0.0	$N_b = 0.1$	$N_t = 0.1$	3.7500	1.1250	1.5000	1.1250	0.7500
		0.8	3.7500	1.1250	1.5000	1.1250	0.7500
		1.6	3.7500	1.1250	1.5000	1.1250	0.7500
	$N_t = 0.1$	$N_b = 0.2$	3.7500	1.1250	1.5000	1.1250	0.7500
		0.5	3.7500	1.1250	1.5000	1.1250	0.7500
		1.0	3.7500	1.1250	1.5000	1.1250	0.7500
0.5	$N_b = 0.1$	$N_t = 0.1$	3.7231	1.1253	1.5145	1.1247	0.7421
		0.8	3.7264	1.1253	1.5113	1.1239	0.7408
		1.6	3.7289	1.1253	1.5080	1.1124	0.7399
	$N_t = 0.1$	$N_b = 0.2$	3.7237	1.1252	1.5141	1.1246	0.7419
		0.8	3.7251	1.1252	1.5127	1.1245	0.7413
		1.2	3.7272	1.1252	1.5104	1.1243	0.7405

Table 3
Thermal characteristics at the interface when iteration order is 50.

λ			$\frac{d\theta_1}{dy}(-1)$	$\theta_1(0)$	$\frac{d\theta_1}{dy}(0)$	$\theta_2(1)$	$\frac{d\theta_2}{dy}(1)$
0.0	$N_b = 0.1$	$N_t = 0.2$	2.4537	0.6458	0.2747	0.8152	0.2051
		0.5	2.4670	0.6607	0.2929	0.8305	0.1957
		1.0	2.4824	0.6780	0.3140	0.8481	0.1850
	$N_t = 0.01$	$N_b = 0.4$	2.4427	0.6335	0.2597	0.8022	0.2130
		0.8	2.4112	0.5982	0.2165	0.7638	0.2365
		1.2	2.3649	0.5463	0.1530	0.7036	0.2733
0.5	$N_b = 0.4$	$N_t = 0.1$	2.4496	0.6469	0.2720	0.8147	0.2036
		0.5	2.3793	0.5671	0.1751	0.7267	0.2572
		0.0	2.3196	0.4996	0.0933	0.6420	0.3088
	$N_t = 0.01$	$N_b = 0.4$	2.4388	0.6346	0.2571	0.8018	0.2115
		0.8	2.4077	0.5994	0.2143	0.7635	0.2348
		1.2	2.3620	0.5476	0.1514	0.7034	0.2713

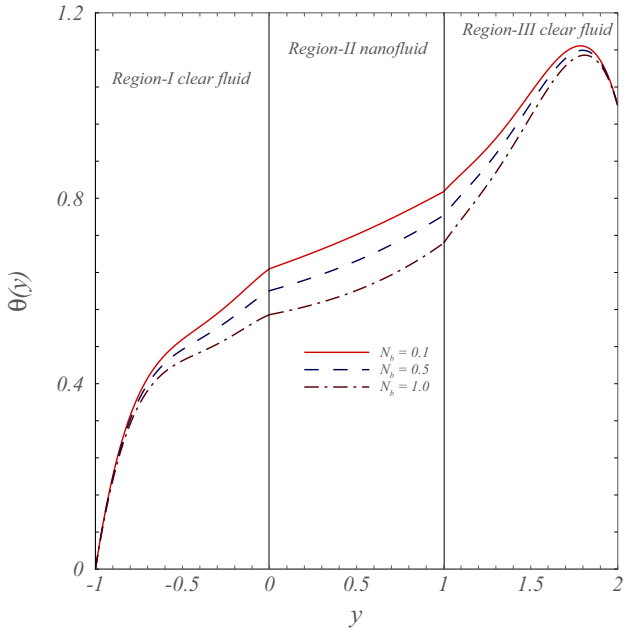

Fig. 3. Temperature profiles for various values of N_b.

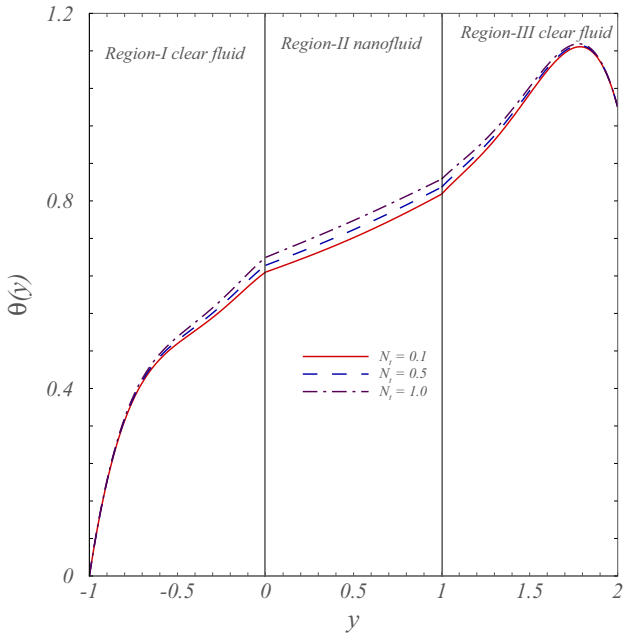

Fig. 4. Temperature plots for different N_t.

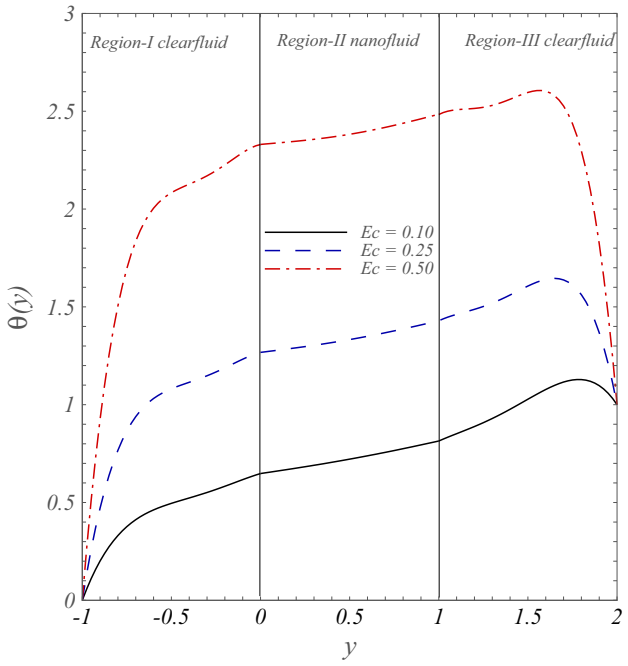

Fig. 5. Temperature plots for different *Ec*.

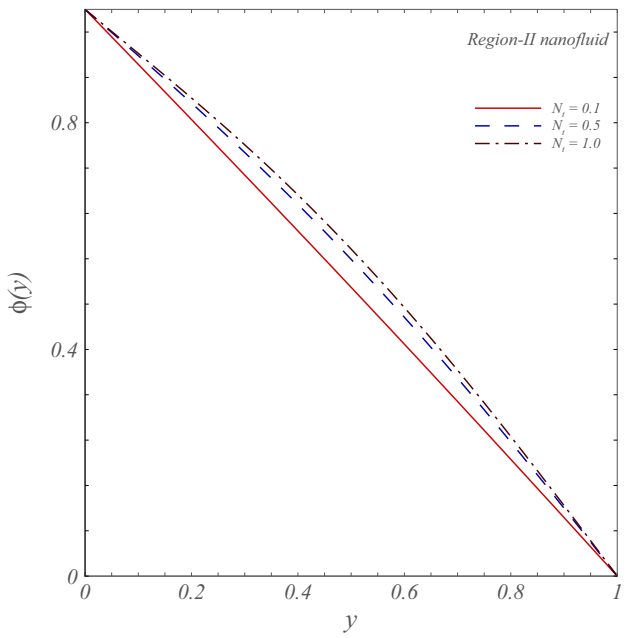

Fig. 6. Concentration profiles for various values of N_t.

temperature is zero at the left end point and finally it approaches to the value of unity at the right end. It demonstrates the influence of N_b on temperature profile. An increase in N_b reduces the temperature in all regions. However the effect is more pronounced in nanofluid region. The effects of N_t on temperature distribution is shown in Fig. 4. The general trend is that the temperature increases and it achieves its maximum value near the right wall in the channel also the increase in N_t enhances the temperature throughout the channel. Larger values of N_t increases the temperature throughout the channel. Fig. 5 describes the temperature distribution for various Eckert numbers. The analysis of graph reveals increasing *Ec* increase the temperature throughout the channel. In Figs. 6 and 7 the general trend of the concentration profile is unity at the left wall of the channel and it approaches to zero at right wall of the channel. An increase in the values of N_b and *Ec* is to increase the width of the nanoparticle volume fraction and hence concentration profile.

4. Conclusions

BVPh2.0 is used to study the three layer fluid model. Due to the importance of multi-layer flows in many industrial processes physically the study might have important application in future. Mathematically this work demonstrate the effectiveness and reliability

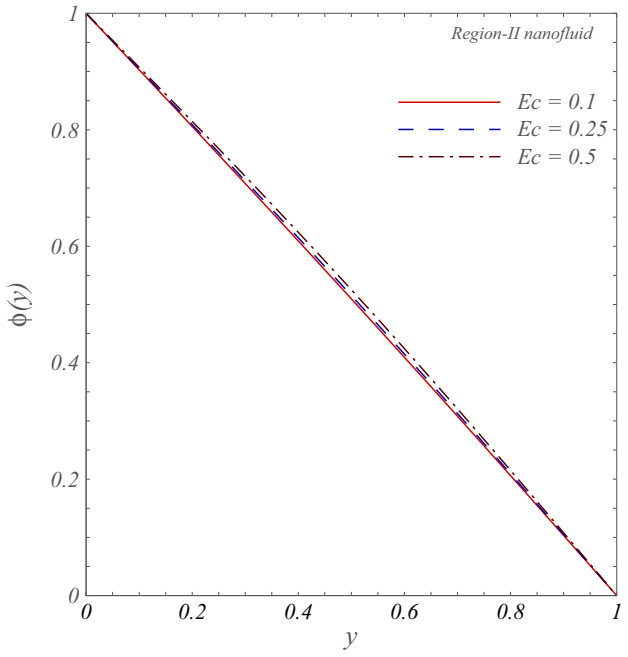

Fig. 7. Concentration profiles for various values of *Ec*.

of BVPh2.0 for nonlinear ordinary differential systems. The important findings are listed below:

[1] The reversed flow phenomenon is observed and the extent of the reversed flow region lies in the center of each layer.
[2] Larger values of the Brownian motion parameter decrease the temperature in all regions. Especially in the nanofluid region the contraction is much faster while quite opposite is true for N_t.
[3] Temperature is an increasing function of Eckert number in all the regions.
[4] Thermophoresis and Eckert number on the concentration have qualitatively similar behavior.

Conflict of interest

Authors declare that there is no conflict of interest.

References

[1] J.C. Maxwell, A Treatise on Electricity and Magnetism, Clarendon Press, 1873.
[2] S.U. Choi, Enhancing thermal conductivity of fluids with nanoparticles, developments and applications of non-newtonian flows, AJME, FED-Vol 231/MD 66 (1995) 99–105.
[3] J. Buongiorno, Convective tranport in nanofluids, ASME J. Heat Transfer 128 (2006) 240–250.
[4] A.V. Kuznetsov, D.A. Nield, Natural convective boundary layer flow of a nanofluid past a verticle plate, Int. J. Therm. Sci. 49 (2010) 243–247.
[5] X.Q. Wang, A.S. Mujundar, A review on nanofluids – Part I: Theoretical and numerical investigations, Braz. J. Chem. Eng. 25 (2008) 613–630.
[6] S.K. Das, S.U. Choi, W. Yu, T. Pardeep, Nanofluids: Science and Technology, Wiley, New Jersey, 2007.
[7] M.M. Rashidi, S. Abelman, N.F. Mehr, Entropy generation in steady MHD flow due to a rotating porous disk in a nanofluid, Int. J. Heat Mass Transfer 62 (2013) 515–525.
[8] I.M. Mahbubul, R. Saidur, M.A. Amalina, Latest developments on the viscosity of nanofluids, Int. J. Heat Mass Transfer 55 (2012) 874–885.
[9] M. Sheikholeslami, R. Elahi, Three dimensional mesoscopic simulation of magnetic field effect on natural convection of nanofluid, Int. J. Heat Mass Transfer 89 (2015) 799–808.
[10] M. Sheikholeslami, T. Hayat, T. Alsaedi, MHD free convection of Al_2O_3-water nanofluid considering thermal radiation: a numerical study, Int. J. Heat Mass Transfer 96 (2016) 513–524.
[11] M. Sheikholeslami, S. Abelman, D.D. Ganji, Numerical simulation of MHD nanofluid flow and heat transfer considering viscous dissipation, Int. J. Heat Mass Transfer 79 (2014) 212–222.
[12] J. Sui, L. Zheng, X. Zhang, G. Chen, Mixed convection heat transfer in power law fluids over a moving conveyor along an inclined plate, Int. J. Heat Mass Transfer 85 (2015) 1023–1033.
[13] H. Xu, I. Pop, Fully developed mixed convection flow in a vertical channel filled with nanofluids, Int. Commun. Heat Mass Transfer 39 (2012) 1086–1092.
[14] M. Sheikholeslami, T. Hayat, T. Alsaedi, On simulation of nanofluid radiation and natural convection in an enclosure with elliptical cylinders, Int. J. Heat Mass Transfer 115 (2017) 981–991.
[15] H. Xu, T. Fan, I. Pop, Analysis of mixed convection flow of a nanofluid in a vertical channel with the buongiorno mathematical model, Int. Commun. Heat Mass Transfer 44 (2013) 15–22.
[16] M. Waqas, M. Farooq, M.I. Khan, A. Alsaedi, T. Hayat, T. Yasmeen, Magnetohydrodynamic (MHD) mixed convection flow of micropolar liquid due to nonlinear stretched sheet with convective condition, Int. J. Heat Mass Transfer 102 (2016) 766–772.
[17] C. Zhang, L. Zheng, X. Zhang, G. Chen, MHD flow and radiation heat transfer of nanofluids in porous media with variable surface heat flux and chemical reaction, Appl. Math. Model. 39 (2015) 165–181.
[18] Y. Lin, L. Zheng, X. Zhang, L. Ma, G. Chen, MHD pseudo-plastic nanofluid unsteady flow and heat transfer in a finite thin film over stretching surface with internal heat generation, Int. J. Heat Mass Transfer 84 (2015) 903–911.
[19] L.N. Tao, On combined free and forced convection in channels, ASME J. Heat Transfer 82 (1960) 233–238.
[20] W. Aung, G. Worku, Developing flow and flow reversal in a vertical channel with asymmetric wall temperature, ASME J. Heat Transfer 108 (1986) 299–304.
[21] T. Kimura, N. Heya, M. Takeuchi, H. Isomi, Natural convection heat transfer phenomena in an enclosure filled with two stratified fluids, Jpn. Soc. Mech. Eng. 52 (1986) 617–625.
[22] M.M. Rashidi, M. Ferdows, J. Uddin, O. Beg, N. Rahimzadeh, Group theory and differential transform analysis of mixed convective heat and mass transfer from a horizontal surface with chemical reaction effects, Chem. Eng. Commun. 199 (8) (2012) 1012–1043.
[23] F. Garoosi, B. Rohani, M.M. Rashidi, Two-phase mixture modelling of mixed convection of nanofluids in a square cavity with internal and external heating, Powder Technol. 275 (2015) 304–321.
[24] O. Beg, M.J. Uddin, M.M. Rashidi, N. Kavyani, Double-diffusive radiative magnetic mixed convective slip flow with Biot and Richardson number effects, J. Eng. Thermophys. 23 (2) (2014) 75–97.
[25] M.M. Rashidi, M. Nasiri, M. Khezerloo, N. Laraqi, Numerical investigation of magnetic field effect on mixed convection heat transfer of nanofluid in a channel with sinusoidal walls, J. Magn. Magn. Mater. 93 (2016) 674–682.
[26] P.M. Patil, D.N. Latha, S. Roy, E. Momoniat, Double diffusive mixed convection flow from a vertical exponentially stretching surface in presence of the viscous dissipation, Int. J. Heat Mass Transfer 112 (2017) 758–766.
[27] A. Altunkaya, M. Avci, O. Aydin, Effects of viscous dissipation on mixed convection in a vertical parallel plate microchannel with asymmetric uniform wall heat fluxes: the slip regime, Int. J. Heat Mass Transfer 111 (2017) 495–499.
[28] S.M. Ibrahim, G. Lorenzini, P.V. Kumar, C.S.K. Raju, Influence of chemical reaction and heat source on dissipative MHD mixed convection flow of a casson nanofluid over a nonlinear permeable stretching sheet, Int. J. Heat Mass Transfer 111 (2017) 346–355.
[29] S. Malik, A.K. Nayak, MHD convection and entropy generation of nanofluid in a porous enclosure with sinusoidal heating, Int. J. Heat Mass Transfer 11 (2017) 329–345.
[30] H. Chen, H. Tseng, S.W. Jhu, J.R. Chang, Numerical and experimental study of mixed convection heat transfer and fluid flow characteristics of plate-fin heat sinks, Int. J. Heat Mass Transfer 11 (2017) 1050–1062.
[31] M.T. Al-Asadi, H.A. Mohammed, A.Sh. Kherbeet, A.A. Al-Aswadi, Numerical study of assisting and opposing mixed convective nanofluid flows in an inclined circular pipe, Int. J. Heat Mass Transfer 85 (2017) 81–91.
[32] S. Farooq, T. Hayat, A. Alsaedi, B. Ahmad, Numerically framing the features of second order velocity slip in mixed convective flow of sisko nanomaterial considering gyrotactic microorganisms, Int. J. Heat Mass Transfer 112 (2017) 521–532.
[33] T. Wang, Z. Wang, Xi. Guang, Zhu. Huang, Periodic unsteady mixed convection in square enclosure induced by inner rotating circular cylinder with time-periodic pulsating temperature, Int. J. Heat Mass Transfer 111 (2017) 1250–1259.
[34] P.M. Patil, A. Shahshikant, S. Roy, E. Momoniat, Unsteady mixed convection over an exponentially decreasing external flow velocity, Int. J. Heat Mass Transfer 111 (2017) 643–650.
[35] J.C. Umavathi, I.C. Liu, J.P. Kumar, D.S. Meera, Unsteady flow and heat transfer of porous media sandwiched between viscous fluids, J. Appl. Math. Mech. Engl. Ed. 31 (12) (2010) 1497–1516.
[36] R.A.V. Gorder, K.V. Prasad, K. Vajravelu, Convective heat transfer in the vertical channel flow of a clear fluid adjacent to a nanofluid layer: a two-fluid model, Heat Mass Transfer (2012), https://doi.org/10.1007/s00231-021-0973-2.
[37] U. Farooq, Z. Lin, Nonlinear heat transfer in a two-layer flow with nanofluids by OHAM, ASME J. Heat Transfer (2013) 56, https://doi.org/10.1115/1.4025432.

[38] U. Farooq, T. Hayat, A. Alsaedi, S. Liao, Heat and mass transfer of a two-layer flows of third-grade nanofluids in a vertical channel, Appl. Math. Comput. 242 (2014) 528–540.
[39] K. Vajravelu, K.V. Prasad, S. Abbasbandy, Convective transport of nanoparticle in multi-layer fluid flow, Appl. Math. Mech. 34 (2) (2013) 177–188.
[40] J.C. Umavathi, I.C. Liu, J.P. Kumar, D.S. Meera, Unsteady flow and heat transfer of porous media sandwiched between viscous fluids, Appl. Math. Mech. 31 (12) (2010) 1497–1516.
[41] S. Liao, The proposed homotopy analysis techniques for the solution of nonlinear problems (Ph.D. dissertation), Shanghai Jiao Tong University, Shanghai (in English).
[42] X. Zhong, S. Liao, Analytic solutions of Von Karman plate under arbitrary uniform pressure (I): Equations in differential form, Stud. Appl. Math. 138 (4) (2016).
[43] X. Zhong, S. Liao, Analytic approximations of von karman plate under arbitrary uniform pressure — equations in integral form, Sci. China Phys. Mech. Astron. (2017) 45, https://doi.org/10.1007/s11433-017-9096-1.
[44] X. Zhong, S. Liao, On the homotopy analysis method for backward/forward-backward stochastic differential equations, Numer. Algorith. 76 (2) (2016).
[45] S. Liao, An optimal homotopy analysis approach for strongly nonlinear differential equaitons, Commun. Nonlinear Sci. Numer. Simul. (2010) 15.
[46] U. Farooq, Y.L. Zhao, T. Hayat, A. Alsaedi, S.J. Liao, Application of the HAM-based mathematica package BVPh2.0 on MHD Falkner-Skan flow of nanofluid, Comput. Fluids 111 (2015) 69–75.
[47] S. Nadeem, R. Mehmood, N.S. Akbar, Optimized analytical solution for oblique flow of a casson-nano fluid with convective boundary conditions, Int. J. Therm. Sci. 78 (2014) 90–100.
[48] S.I. Khan, S.T. Mohyud-Din, Y. Xiao-Jun, Squeezing flow of micropolar nanofluid between parallel disks, J. Magn. 21 (3) (2016) 476–489.
[49] Z. Jing, D. Yang, L.C. Zheng, X.X. Zhang, Second-order slip effects on heat transfer of nanofluids with reynolds model of viscosity in a coaxial cylinder, Int. J. Nonlinear Sci. Numer. Simul. 16 (6) (2015) 285–292.
[50] Z. Jing, D. Yang, L.C. Zheng, X.X. Zhang, Effects of second order velocity slip and nanoparticles migration on flow of buongiorno nanofluid, Appl. Math. Lett. 52 (2016) 183–191.